

Article

Inflorescence Trait Diversity and Genotypic Differentiation as Influenced by the Environment in *Elymus nutans* Griseb. from Qinghai–Tibet Plateau

Jin Li ^{1,2,†} , Haoqi Tian ^{3,†}, Wenqin Ji ¹, Changbing Zhang ⁴ and Shiyong Chen ^{1,2,*}¹ College of Animal and Veterinary Sciences, Southwest Minzu University, Chengdu 610041, China² Sichuan Zoige Alpine Wetland Ecosystem National Observation and Research Station, Southwest Minzu University, Chengdu 610041, China³ Key Laboratory of Superior Forage Germplasm in the Qinghai–Tibetan Plateau, Qinghai Academy of Animal Science and Veterinary Medicine, Qinghai University, Xining 810016, China⁴ Sichuan Academy of Grassland Science, Chengdu 611731, China

* Correspondence: chensy@swun.edu.cn; Tel.: +86-28-85522310

† These authors contributed equally to this work.

Abstract: The alpine forage grass species *Elymus nutans* Griseb. is widely distributed in the Qinghai–Tibet Plateau and the Himalayas due to its high adaptability. However, it has become threatened by climate warming and excessive grazing. Thus, understanding its genetic and phenotypic information is crucial to aid resource management and conservation efforts. In this study, microsatellite markers were developed based on RNA-seq transcriptome data from *E. nutans* Griseb. varieties ‘Aba’ and ‘Kangbei’, resulting in the identification of 48,457 SSRs from 304,554 de novo assembled unigenes. Seventeen polymorphic markers, 13 inflorescence phenotypic traits, and seed shattering values were determined for 31 *E. nutans* accessions collected from eastern Tibet. The molecular markers generated 134 well-amplified bands with a mean Nei’s genetic diversity of 0.31 and a Shannon information index of 0.46. Pairwise genetic similarity ranged from 0.554 to 0.895, with an average of 0.729. Based on the molecular marker data, all accessions were divided into two classes via the unweighted pair-group method with arithmetic mean (UPGMA), the Markov chain Monte Carlo method, and the principal coordinate analysis (PCA) method. We used Tassel analysis to determine 11 loci with a significant relationship to phenotypic traits, and Pearson’s correlation analysis showed that some inflorescence traits were significantly influenced by the environment. Furthermore, we detected strong patterns of isolation by both environment (IBE) and distance (IBD) via Mantel analysis. This study provides valuable insights into the genetic and phenotypic differentiation of *E. nutans*, informing germplasm resource evaluation and future breeding.

Keywords: *Elymus nutans*; Qinghai–Tibet plateau; transcriptome; genetic diversity; phenotypic differentiation; isolation patterns



Citation: Li, J.; Tian, H.; Ji, W.; Zhang, C.; Chen, S. Inflorescence Trait Diversity and Genotypic Differentiation as Influenced by the Environment in *Elymus nutans* Griseb. from Qinghai–Tibet Plateau. *Agronomy* **2023**, *13*, 1004. <https://doi.org/10.3390/agronomy13041004>

Academic Editors: Jiejun Xi, Aike Bao, Linkai Huang, Bin Xu, Shangang Jia and Peng Zhou

Received: 2 March 2023

Revised: 25 March 2023

Accepted: 28 March 2023

Published: 29 March 2023



Copyright: © 2023 by the authors. Licensee MDPI, Basel, Switzerland. This article is an open access article distributed under the terms and conditions of the Creative Commons Attribution (CC BY) license (<https://creativecommons.org/licenses/by/4.0/>).

1. Introduction

With the continuous growth of the world population (<http://esa.un.org/unpd/wpp/index.htm>, accessed on 1 January 2022), determining how to increase the global crop yield has become an urgent challenge. The Triticeae tribe includes several important cereal crops and forage grasses, which are the main sources of food for humans and livestock [1], including *Elymus* [2], *Leymus* [3], and *Bromus* [4] that possess desirable resistance and character traits and therefore constitute a valuable gene pool for wheat grains. The collection and evaluation of the genetic diversity of these forage germplasm resources are of great significance for forage and crop breeding. *Elymus nutans* Griseb., a perennial, cespitose, self-pollinating, allohexaploid ($2n = 6x = 42$) species [5], is an important alpine forage species in the genus *Elymus* that is widely distributed at an altitude of 3000–4500 m in the Qinghai–Tibet Plateau (QTP) and the Himalayas [6,7]. Because of its high yield, nutrient richness,

and high adaptability to various abiotic stressors, it is used for ecological restoration and the construction of artificial grasslands and is regarded as a species suitable for the study of agriculture and ecology in the QTP [8]. *Elymus nutans* also plays a vital role in animal husbandry and environmental maintenance. However, in recent decades, climate change and overgrazing have threatened the habitat of indigenous plants in the QTP region [9], which has affected the distribution and growth of many plants, including *Elymus sibiricus* [10], *Meconopsis punicea* [11], and *Hippophaë neurocarpa* [12]. Even *E. nutans*, the dominant species, has been affected [13]. Conserving wild *E. nutans* germplasm resources is imperative to maintaining ecosystem stability, and understanding the genetic and geographical differentiation of this germplasm is a prerequisite for the implementation of conservation programs and is of great significance to breeding studies.

The genetics of *E. nutans* have been studied using methods including inter-simple sequence repeat markers (ISSRs) [14], gliadins [15], amplified fragment length polymorphisms (AFLPs) [16], and simple sequence repeats (SSRs) [13]. These studies have demonstrated the wide genetic basis of *E. nutans* resources. With the advancement of next-generation transcriptome sequencing techniques, expressed sequenced tag (EST)-SSR markers have been widely used due to their high polymorphism, transferability, and tight linkage with functional genes [17,18]. These SSR markers have been applied to various forage grass species in recent years, including *Elymus sibiricus* [19], *Kengyilia melanthera* [20], and *Bromus catharticus* [21]. In the case of *E. nutans*, Luo et al. analyzed de novo transcriptome sequencing data from different tissues and developed a large number of EST-SSR markers [22], whereas Zhao et al. conducted a comparative transcriptome analysis to explore candidate genes related to seed shattering [23], providing valuable resources for exploring genetic variation and molecular marker-assisted breeding.

The integration of phenotypic evaluation with molecular marker evaluation is of utmost significance. Linkage disequilibrium (LD) association analysis can identify the marker–trait relationship among individuals, which is invaluable for molecular marker-assisted breeding [24] and has been successfully applied to wheat and other important crops and forages [25,26]. In addition, the correlation between phenotypes and environmental conditions can provide insight into a species' adaptability to its local environment [27], thus facilitating the comprehensive evaluation of plant germplasm resources. Moreover, the integration of phenotypic, genetic, and environmental variations contributes to the understanding of population differentiation and speciation [28]. Plant genetic and phenotypic differentiation within natural populations may be affected by natural selection, genetic drift, geographical isolation, and other factors [29]. According to conventional perspectives, as distance increases, the decrease in gene flow between populations results in genetic differentiation, referred to as isolation by distance (IBD) [30]. By contrast, gene flow reduction due to local adaptation to differing environments is referred to as isolation by ecology or the environment (IBE) [31]. Despite a growing number of studies on the genetic differentiation patterns of grass species [20,32], research on *E. nutans* has been limited, hindering the utilization and preservation of its resources.

Therefore, to better understand the current situation of *E. nutans* germplasm resources, we developed new EST-SSR markers based on RNA-seq to obtain genetic information about *E. nutans* from Tibet and to analyze their genetic differentiation patterns. The Tibetan plateau is an ideal location to study genetic variation due to its high elevation and the changeable climate on a small scale [33]. In this study, we evaluated 31 *E. nutans* germplasm resources by comprehensively identifying SSR loci and developing new molecular markers based on the transcriptome. We also generated genotypic, phenotypic, geographical, and climatic data to explore the effects of IBD and IBE on genetic differentiation processes.

2. Materials and Methods

2.1. Transcriptome Sequencing and EST-SSR Design

E. nutans Griseb. cv. 'Aba' and 'Kangbei', two genotypic varieties with different tiller types, were used for transcriptome sequencing analysis. Transcriptome sequencing of

the two varieties was conducted through the isolation of total RNA from fresh young leaves using a Plant Total RNA Kit (Tiangen Biotech Co., Ltd., Beijing, China) following the manufacturer's protocol. Then, the quality of the RNA was assessed using an Agilent Bioanalyzer 2100 (Agilent Technologies, Palo Alto, CA, USA), and its integrity was confirmed through 1% agarose gel electrophoresis. The cDNA library was generated using a NEBNext Ultra RNA Library Prep Kit for Illumina (NEB, San Diego, CA, USA) and quantified using Qubit 2.0. The insert size of the library was evaluated using an Agilent Bioanalyzer 2100. High-throughput sequencing of the library was performed on the Illumina HiSeq platform, generating paired-end reads. Adapter contaminants were removed from the sequencing reads to obtain clean reads. The quality reads were then subjected to de novo transcriptome assembly using the Trinity program [34].

The presence of SSR markers among the assembled unigene sequences was identified using the MicroSatellite (MISA) identification tool [35]. The EST-SSR primers were designed using Primer 3 software (<http://primer3.sourceforge.net>, accessed on 26 January 2019) based on the results from MISA. Finally, 100 designed EST-SSR primer pairs were synthesized using Tingke Biological Technology (Beijing, China).

2.2. Plant Materials and DNA Extraction

A total of 31 populations of *E. nutans* were sampled from Eastern Tibet (Figure 1, sampling information was listed in Supplementary Table S1), including Qamdo (QD), Nyingchi (NC), Lhasa (LS), and Nagqu (NQ), with 10 individuals per population, a distance of at least 5 m was maintained between each individual to avoid sampling similar genotypes. The sample seeds were planted in the experimental field at the Sichuan Academy of Grassland Sciences (latitude: 32.78° N; longitude: 102.54° E; altitude: 3502 m) in November 2018. In the following year, fresh leaf tissues from 10 individuals per population were mixed in equal amounts, dried in zip-lock plastic bags containing silica gel, and stored for DNA extraction. Total genomic DNA was extracted using a DP350 Plant DNA kit (Tiangen Biotech Co., Ltd., Beijing, China) following the manufacturer's instructions. The quality and concentration of the extracted DNA were evaluated using 1% agarose gel electrophoresis and NanoDrop-Lite (Thermo Scientific, Waltham, MA, USA). The DNA was then diluted to a concentration of 10 ng/μL and stored at −20 °C.

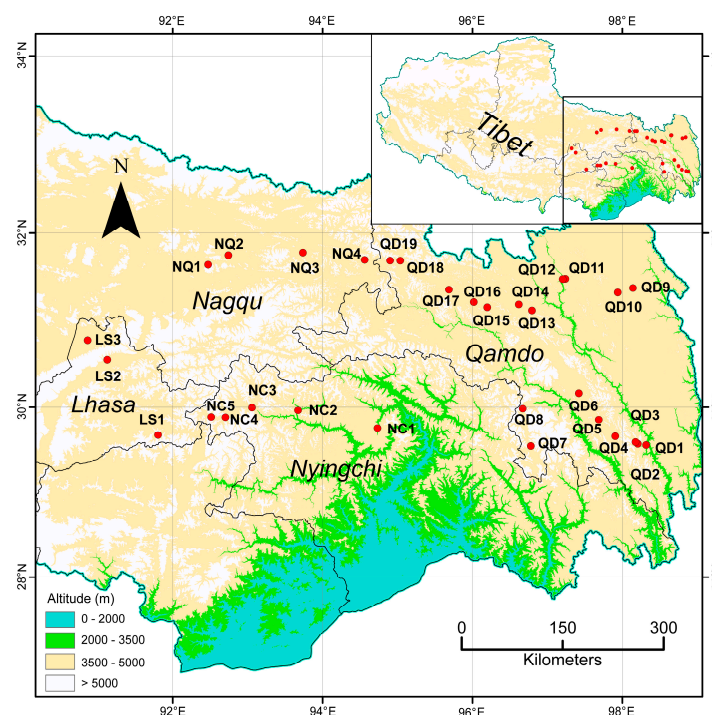


Figure 1. The geographical locations of 31 populations of *Elymus nutans*.

2.3. Genetic Diversity Analysis

PCR amplification was carried out in a 20 μ L reaction volume, containing 20 ng of genomic DNA, 0.5 μ M of each primer, and 10 μ L of 2 \times Es Taq MasterMix (Dye Plus) (CoWin Biosciences, Beijing, China). A PTC-200 Thermal Cycler (BIO-RAD, Hercules, CA, USA) was used for a touch-down PCR reaction under the program of 94 $^{\circ}$ C for 4 min, 1 cycle; 94 $^{\circ}$ C for 30 s, 65–60 $^{\circ}$ C for 30 s, 72 $^{\circ}$ C for 60 s, 5 cycles; 94 $^{\circ}$ C for 30 s, 60 $^{\circ}$ C for 30 s, 72 $^{\circ}$ C for 60 s, 35 cycles; 72 $^{\circ}$ C for 10 min, 1 cycle; and 4 $^{\circ}$ C indefinitely. The PCR products were separated on 6% non-denaturing polyacrylamide gel electrophoresis and stained with silver staining. The EST-SSR profiles obtained for each accession were scored as present (1) or absent (0) and transformed into a 1/0 matrix for further analysis. We calculated certain genetic diversity parameters, including percentages of polymorphic bands (PPB), Nei's genetic diversity (H), and the Shannon information index (I), using POPGENE1.32 [36]. The dendrogram was constructed using the unweighted pair-group method with arithmetic mean (UPGMA) clustering through Nei–Li's similarity coefficients and drawn using MEGA v6.0 software [37]. A model-based Bayesian clustering approach was used to analyze the genetic structure and define the most likely number of clusters (K) using STRUCTURE v.2.3.4 software [38] and the Structure Harvester website [39]. Principal coordinate analysis (PCoA) and Nei's genetic distance were carried out using the GenAlEx 6.5102 project [40].

2.4. Phenotypic Variation and Association Analysis

A total of 310 individual plants were selected during the filling period in August 2021 for evaluating inflorescence phenotypic traits. We measured the spikelet number (SKN), spikelet length (SKL), outer glume length (OGL), outer glume width (OGW), outer glume awn length (OGAL), inner glume length (IGL), inner glume width (IGW), inner glume awn length (IGAL), outer lemma length (OLL), outer lemma width (OLW), outer lemma awn length (OLAL), inner lemma length (ILL), and inner lemma width (ILW) to estimate phenotypic differentiation among accessions, and these quantitative traits were measured in millimeters. Seed shattering values for each accession were determined at the milk-ripe stage by testing the pedicel-breaking tensile strength (BTS) (g) using 50 seeds per population. In addition, bioclimatic data were acquired from the WorldClim website (<https://www.worldclim.org/>, accessed on 20 June 2021) and analyzed using ArcGIS10.2 (ESRI, Inc., Redlands, CA, USA) to investigate the impact of bioclimatic and geographical factors on seed shattering and inflorescence phenotypic traits. The associations between the EST-SSRs and the inflorescence phenotypic traits and BTS values were then analyzed through a general linear model (GLM) implemented in Tassel software 5.0 [41].

2.5. Genetic and Phenotypic Differentiation Analysis

The Mantel test was used to detect possible isolation patterns of *E. nutans* accessions from different regions. The phenotypic distance between accessions was defined as their inflorescence phenotypic Euclidean distance. Furthermore, the geographic and climatic distances between the 31 sampling sites were calculated using latitude and longitude data obtained in the field and 19 standard bioclimatic variables from the WorldClim website. The relationship between genetic distance and geographical distance was evaluated to test the IBD hypothesis. The effect of environmental distance was interchanged with geographical distance to test the hypothesis of IBE. Moreover, the possibility of phenotypic differentiation caused by climatic and geographic distances was also explored.

3. Results

3.1. De Novo Assembly and Distribution of SSR Repeats

After undergoing Illumina sequencing and quality filtering, a total of 62,653,976 and 66,395,430 clean reads were obtained for cv. 'Aba' and cv. 'Kangbei', respectively, amounting to approximately 9.4 and 9.96 Gb of data, respectively. These clean reads were submitted to the NCBI's Sequence Read Archive database under BioProject ID: PRJNA934126. The clean reads were then mixed and de novo assembled using Trinity software, resulting in

434,637 transcripts with an N50 length of 1062 bp, an N90 length of 337 bp, and a mean length of 753 bp (transcripts shorter than 200 bp were discarded). As the length of the transcripts increased, the number of transcripts decreased (Table 1). The transcripts were further clustered into 304,554 unigenes with a mean length of 931 bp, an N50 length of 1194 bp, and an N90 length of 478 bp (Table 1).

Table 1. Overview of de novo sequence assembly for *E. nutans*.

Length Range (bp)	Transcripts	Unigene
200–500	205,785	88,679
500–1000	123,056	111,828
1000–2000	83,850	82,173
>2000	21,973	21,874
Total Number	434,637	304,554
Total Length	327,236,286	283,614,840
N50 Length	1062	1194
N90 Length	337	478
Mean Length	753	931

Using MISA software, a total of 48,457 SSRs were identified from 41,444 SSR-containing sequences, with trinucleotide repeats being the most abundant type (43.06%), followed by mononucleotide (32.54%), dinucleotide (21.25%), tetranucleotide (2.46%), pentanucleotide (0.45%), and hexanucleotide (0.24%) (see Table 2). Among the dinucleotide repeats, AG/CT (5924) was the most dominant, followed by AC/GT (2593) and AT/TA (1174). CCG/CGG (8378), AGG/CCT (3618), and AGC/CTG (3287) made up 73.2% of all trinucleotide repeat repeats. ATCC/ATGG (107), AGAGG/CCTCT (33), and AAGAGG/CCTCTT (9) dominated the tetranucleotide, pentanucleotide, and hexanucleotide repeats, respectively, although they were rare (Supplementary Table S2). In addition, the repeat times of SSR repeats were distributed from 5 to 83 times, and the repeat times of mononucleotides were more than nine times. The main repeat times of dinucleotides, trinucleotides, and tetranucleotides were six, five, and five times, respectively.

Table 2. The distribution of EST-SSRs based on the number of repeat units.

Number of Repeat Units	Mono-	Di-	Tri-	Tetra-	Penta-	Hexa-	Total	Percentage (%)
5	0	0	12,830	860	198	79	13,967	28.82
6	0	3733	4731	272	11	23	8770	18.10
7	0	1784	2002	31	9	7	3833	7.91
8	0	1131	870	17	2	7	2027	4.18
9	0	742	158	6	0	1	907	1.87
10	6017	501	112	4	0	0	6634	13.69
11	2665	476	63	0	0	0	3204	6.61
12	1501	511	39	0	0	0	2051	4.23
13	821	219	19	1	0	0	1060	2.19
14	707	210	16	0	0	0	933	1.93
15	506	195	9	0	0	0	710	1.47
>15	3550	793	18	0	0	0	4361	9.00
Total	15,767	10,295	20,867	1191	220	117	48,457	100.00
Percentage (%)	32.54	21.25	43.06	2.46	0.45	0.24	100.00	

3.2. Genetic Relationship Analysis

To validate the markers identified in this study, 100 pairs of EST-SSR primers were randomly selected and synthesized for validation. First, the primers were tested for PCR amplification in 31 *E. nutans* accessions, and 17 polymorphic SSR primer pairs generated 134 well-amplified bands with consistent sizes. These primers were then used for further analysis. The results revealed a range of 4–12 alleles per primer, with an average of 7.88 and a mean percentage of polymorphic bands (PPB) of 92.54%. Furthermore, Nei's genetic diversity (H) ranged from 0.02 to 0.47, with a mean value of 0.31, and the Shannon information index (I) ranged from 0.04 to 0.66, with a mean of 0.46. In addition, we compared these primers to the genes in the NR and NT libraries and obtained the Genbank ID and corresponding descriptions of these genes (as shown in Supplementary Table S3).

Nei–Li's similarity coefficients were calculated to examine the genetic relationships among the 31 accessions. The coefficients ranged from 0.554 (between QD1 and NQ1) to 0.895 (between QD16 and QD17), with an average of 0.729. We found that the accessions collected from Qamdo showed the highest levels of Nei's genetic diversity ($H = 0.46$) and Shannon information index ($I = 0.31$), while those from Lhasa had the lowest levels of both metrics ($H = 0.19$ and $I = 0.17$; see Supplementary Table S4). Furthermore, a UPGMA dendrogram was constructed based on genetic similarity, which revealed that the 31 germplasm resources were separated into two clusters (Figure 2). However, accessions from the same region were not grouped into the same class. Cluster I consisted of 22 accessions, with 12 from Qamdo, three from Nyingchi, and all from Lhasa and Nagqu, while Cluster II contained nine accessions from Qamdo (7) and Nyingchi (2). Based on the Bayesian model and delta K values, $K = 2$ was unambiguously the most likely number of subgroups (Supplementary Figure S1), and the results of the STRUCTURE analysis when $K = 2$ were consistent with the two UPGMA classes identified (Figure 2). In addition, PCA indicated that all 31 accessions could also be divided into two groups, in agreement with the aforementioned results (Figure 3).

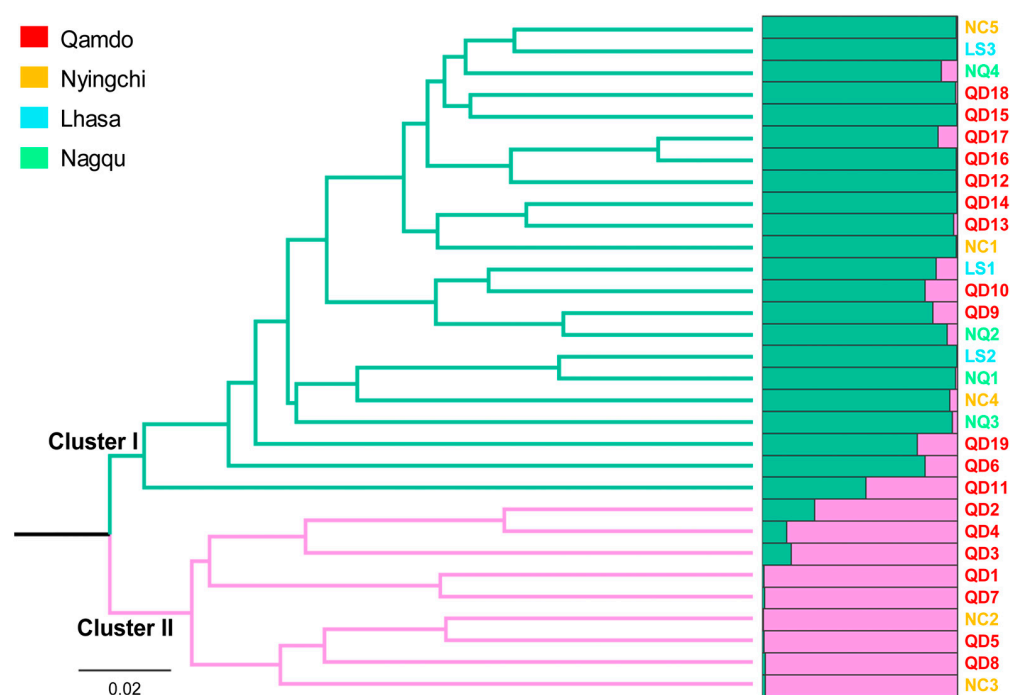


Figure 2. Population structure of 31 *Elymus nutans* accessions based on UPGMA and Bayesian clustering ($K = 2$). All accessions were grouped into two clusters. The accession codes with red, yellow, blue, and green indicate that these accessions were collected from Qamdo, Nyingchi, Lhasa, and Nagqu, respectively. All accessions colored based on the sample origins were divided into two UPGMA clusters and STRUCTURE subgroups.

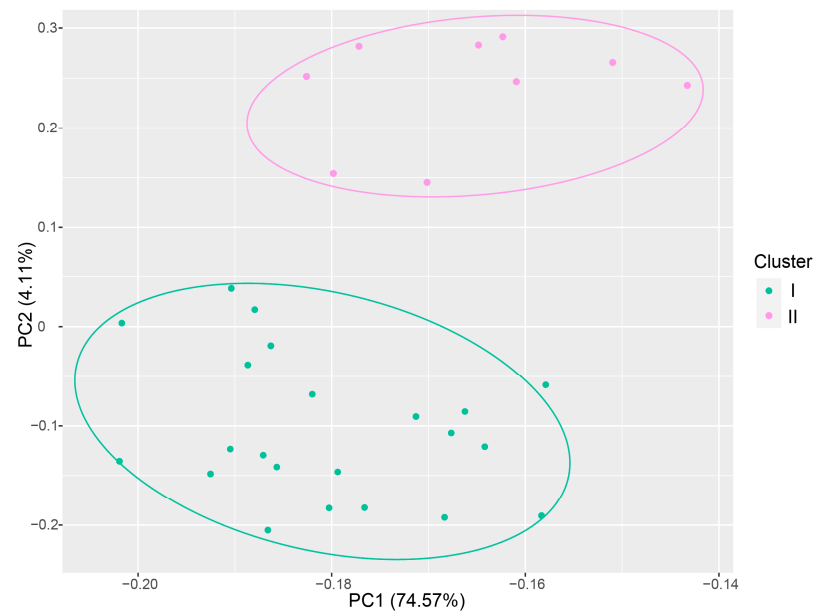


Figure 3. Principal coordinate analysis (PCoA) of 31 *Elymus nutans* accessions based on EST-SSR data.

3.3. Inflorescence Phenotypic Characteristics, Shattering, and Tassel Analysis

In this study, 13 phenotypic traits of *E. nutans* germplasm were analyzed to determine their variability. The germplasm possessed a high degree of phenotypic variation, with variation coefficients ranging from 7.34% to 36.5% and an average of 19.45% (as detailed in Table 3). Moreover, cluster analysis was performed on the phenotypic data, which divided the materials into two distinct clusters (Figure 4). Interestingly, materials from different regions were present in both clusters, suggesting that the observed phenotypic differences were not solely the result of geographical distribution. Further analysis revealed that Cluster II had larger seed characteristics and higher BTS values compared with the materials in Cluster I (Figure 4).

Table 3. Variation analysis of 13 phenotypic characteristics of *E. nutans*.

Quantitative Traits	Mean	Max	Min	SD	Variation Coefficient (%)	Genetic Diversity Index
SKN	42.99	68.80	27.70	7.20	16.74	1.94
SKL (mm)	27.97	40.16	14.16	4.92	17.61	1.88
OGL (mm)	4.62	7.37	3.04	0.74	16.03	1.77
OGW (mm)	0.95	1.30	0.62	0.16	16.94	1.82
OGAL (mm)	1.51	3.07	0.30	0.54	35.50	1.94
IGL (mm)	3.66	5.90	1.53	0.69	19.01	1.92
IGW (mm)	0.79	1.14	0.35	0.17	21.76	2.03
IGAL (mm)	1.23	2.37	0.33	0.45	36.48	2.03
OLL (mm)	9.42	11.46	7.67	0.69	7.34	1.94
OLW (mm)	2.18	3.10	1.60	0.43	19.73	1.63
OLAL (mm)	14.55	21.27	5.43	3.55	24.37	1.97
ILL (mm)	8.75	10.16	6.77	0.71	8.17	1.96
ILW (mm)	1.81	2.37	1.35	0.24	13.15	2.04

SKN, spikelet number; SKL, spikelet length; OGL, outer glume length; OGW, outer glume width; OGAL, outer glume awn length; IGL, inner glume length; IGW, inner glume width; IGAL, inner glume awn length; OLL, outer lemma length; OLW, outer lemma width; OLAL, outer lemma awn length; ILL, inner lemma length; ILW, inner lemma width.

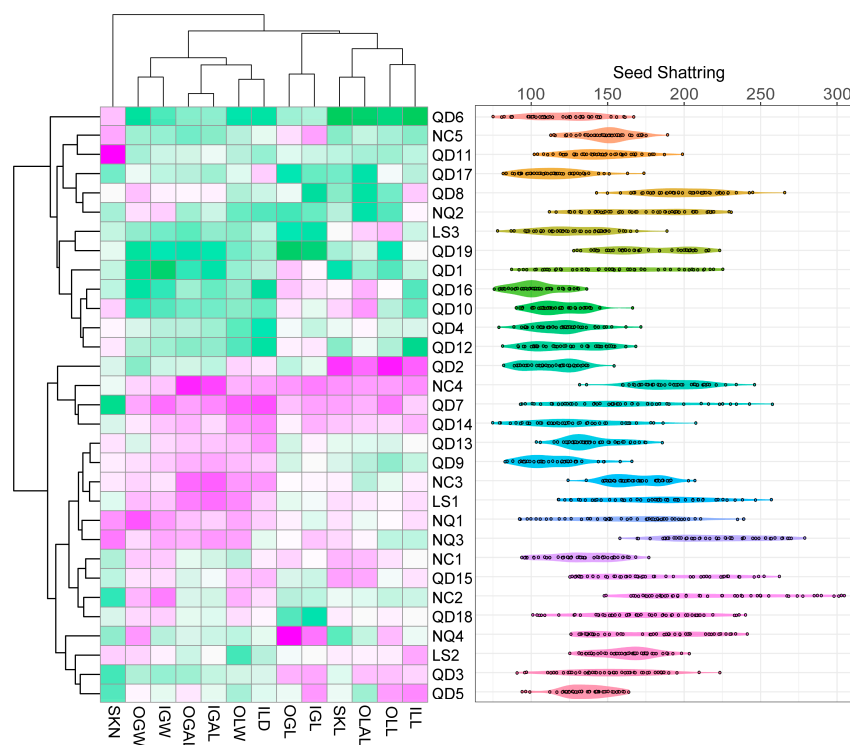


Figure 4. UPGMA cluster of 31 *Elymus nutans* populations based on 13 inflorescence phenotypic traits and corresponding seed-shattering values, the clustering results are shown on the left and the right plot shows the corresponding drop grain properties of each population. SKN, spikelet number; SKL, spikelet length; OGL, outer glume length; OGW, outer glume width; OGAL, outer glume awn length; IGL, inner glume length; IGW, inner glume width; IGAL, inner glume awn length; OLL, outer lemma length; OLW, outer lemma width; OLAL, outer lemma awn length; ILL, inner lemma length; ILW, inner lemma width.

The results of Tassel software based on the GLM model showed that a total of 11 loci amplified by EST-SSR markers had a significant relationship ($p < 0.01$) with the BTS value and 12 phenotypic traits, with the exception of ILW (Table 4). Notably, seven of these traits were significantly associated with two loci amplified by marker EN5.

Table 4. Association analysis for phenotypic traits in the 310 *Elymus nutans* individuals studied using the GLM model.

Trait	Marker	<i>p</i>	Marker_R2	Trait	Marker	<i>p</i>	Marker_R2
BTS	EN48-260 bp	0.00305	0.28356	OGL	EN57-183 bp	0.00084	0.33773
IGAL	EN5-256 bp	0.00019	0.40221	OGL	EN99-150 bp	0.00153	0.31079
IGAL	EN55-256 bp	0.00368	0.26985	OGW	EN5-256 bp	0.00126	0.32361
IGL	EN57-183 bp	0.00975	0.21398	OGW	EN58-243 bp	0.00898	0.22701
IGW	EN5-256 bp	0.00018	0.40794	OLAL	EN5-235 bp	0.00079	0.32793
IGW	EN58-243 bp	0.00967	0.22345	OLL	EN5-235 bp	0.00583	0.23654
ILL	EN35-207 bp	0.00252	0.26241	OLW	EN55-208 bp	0.00888	0.22983
ILL	EN91-239 bp	0.00746	0.21351	SKL	EN5-235 bp	0.00293	0.27998
OGAL	EN5-256 bp	0.00063	0.35446	SKN	EN90-228 bp	0.00567	0.19378
OGAL	EN55-208 bp	0.00594	0.24807	SKN	EN99-164 bp	0.00611	0.19025

BTS, seed shattering; IGAL, inner glume awn length; IGL, inner glume length; IGW, inner glume width; ILL, inner lemma length; OGAL, outer glume awn length; OGL, outer glume length; OGW, outer glume width; OLAL, outer lemma awn length; OLL, outer lemma length; OLW, outer lemma width; SKL, spikelet length; SKN, spikelet number.

In addition, Pearson correlation analysis was performed to evaluate the influence of environmental factors on the phenotypic characteristics. The analysis included longitude (Lon), latitude (Lat), altitude (Alt), 19 bioclimatic variables (Bio1–19), 13 inflorescence phenotypic traits, and the BTS of seeds (as shown in Supplementary Figure S2). The three variables were significantly correlated with the inflorescence characteristics (Figure 5). Specifically, SKN was positively correlated with the mean diurnal range ($r = 0.451$, Figure 5A) and negatively correlated with the precipitation of the wettest month ($r = -0.465$, Figure 5B). Furthermore, BTS and OGW were negatively correlated with Lon ($r = -0.472$ and -0.423 , Figure 5C,D, respectively).

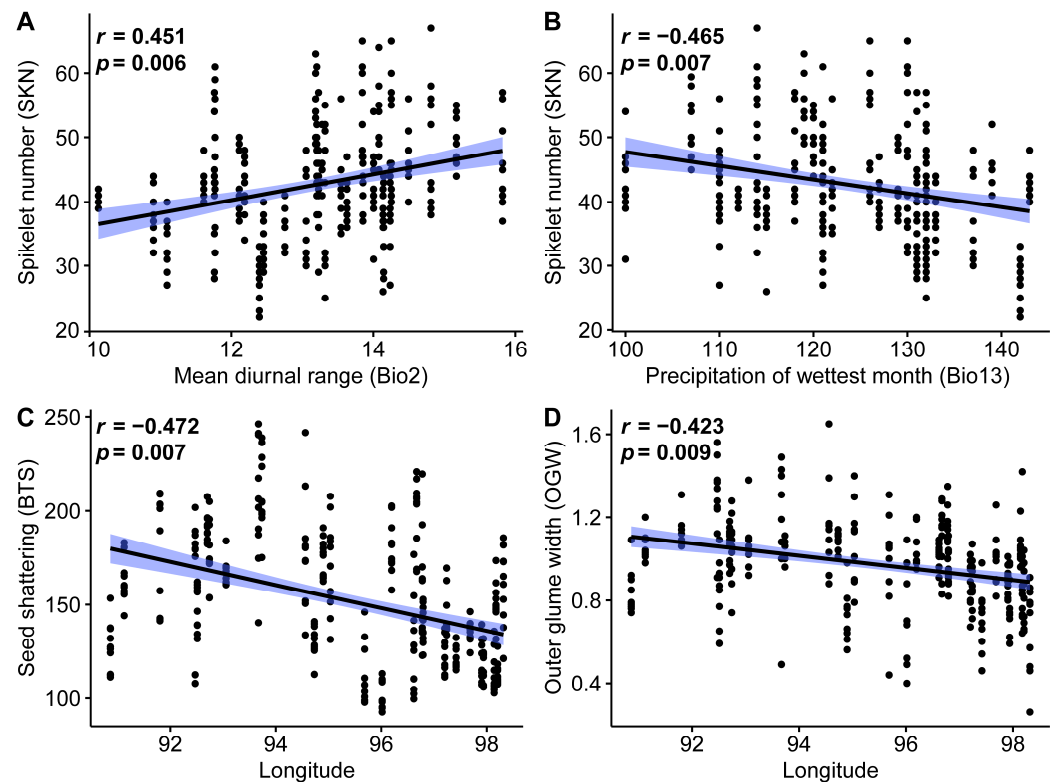


Figure 5. Correlation analysis of environmental and geographical conditions on the inflorescence characteristics of *Elymus nutans*. (A) Regression of mean diurnal range and spikelet number. (B) Regression of Precipitation of wettest month and spikelet number. (C) Regression of longitude and seed shattering. (D) Regression of longitude and outer glume width.

3.4. Associations between Genetic, Phylogenetic, Geographical, and Climatic Distance

Mantel analysis was performed to determine the contributions of geographic and climatic distance between sampling localities to genetic and phenotypic differentiation (Figure 6), which showed that genetic distance had both significant correlations with climatic distance ($r = 0.574$, $p = 0.001$, Figure 6A) and geographic distance ($r = 0.329$, $p = 0.001$, Figure 6B), thus suggesting strong IBE and IBD. However, a significant autocorrelation between geographic and climatic distances was detected (Figure 6C). In addition, no significant correlation was detected for phenotypic distance with climatic distance or geographic distance (Figure 6D,E), indicating that the inflorescence differentiation of *E. nutans* was less driven by geography or environment. A weak but significant positive correlation was detected between genetic distance and phenotypic distance ($r = 0.21$, $p = 0.009$, Figure 6F).

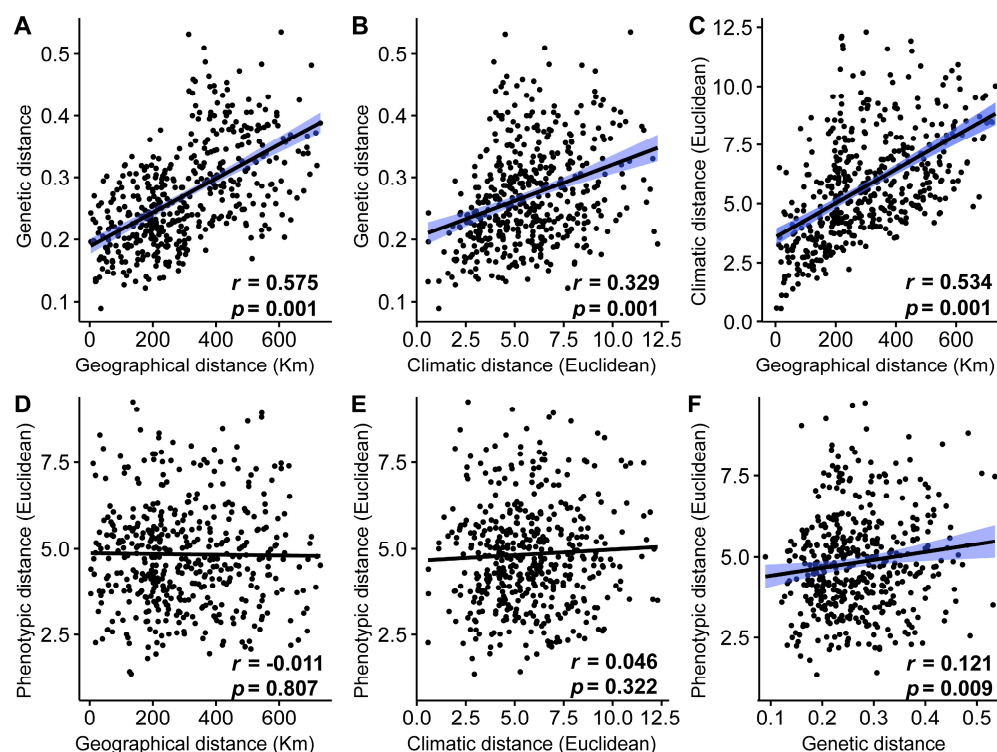


Figure 6. Regression of genetic, phylogenetic, geographical, and climatic distance among all population pairwise comparisons. (A) Regression of geographical and genetic distance. (B) Regression of climatic and genetic distance. (C) Regression of geographical and climatic distance. (D) Regression of geographical and phylogenetic distance. (E) Regression of climatic and phylogenetic distance. (F) Regression of genetic and phylogenetic distance.

4. Discussion

4.1. Characterization of *E. nutans* Transcriptome and EST-SSR Distribution

The alpine forage species *E. nutans* is characterized by exceptional resistance, widely distributed in the QTP, and plays a crucial role in forage production and the ecosystem. Consequently, the analysis of genetic diversity and development of molecular markers for molecular breeding are of paramount importance. In recent years, RNA-Seq based on next-generation sequencing has gained popularity among researchers. In particular, the Illumina platform offers the advantage of rapid, cost-effective, and independent analysis compared with traditional methods. Leveraging the benefits of next-generation sequencing technology, our comprehensive transcriptomic analysis of *E. nutans* was performed in two varieties, resulting in the assembly of 304,554 unigenes, with 264,985 (87%) annotated. This number of assembled unigenes represents a three-fold increase in comparison to previous studies on the same species [22] and is similar to that observed in other recent studies on forage species [21]. The mean length and N50 value of all unigenes were 931 and 1194 bp, respectively, both longer than the corresponding values observed in a previous study on *E. nutans* (635 and 926 bp, respectively) by Luo et al. [22]. The increased length of unigenes enhances the accuracy and efficiency of transcriptome assembly, providing valuable information for investigating gene function and molecular mechanisms.

In recent years, EST-SSR markers have proven to be powerful tools for investigating genetic diversity, characterizing population structure, and facilitating marker-assisted selection in breeding programs [19,42]. Our transcriptomic analysis of two varieties of *E. nutans* revealed a rich resource of SSRs, with a total of 48,457 markers identified. This number is significantly higher than in previous reports, indicating a substantial improvement in the availability of SSR resources for the study of this important grass on the QTP. Our analysis of SSR motifs showed that trinucleotide repeats were the most abundant type

(63.8%), followed by dinucleotide (31.5%) and tetranucleotide (3.6%) repeats. This pattern is consistent with those observed in other plant genomes, such as *E. sibiricus* [19] and *Bromus catharticus* [21], where trinucleotide repeats were the most prevalent motif, comprising 50% and 60% of SSRs, respectively. The CCG/CGG motif was the most predominant trinucleotide repeat in our analysis, consistent with previous findings [21]. Meanwhile, the AG/CT type was the most abundant dinucleotide repeat (%), which was consistent with the patterns of sequence motifs found by Luo et al. in a similar study [22]. In conclusion, the transcriptome data generated in this study represent a more comprehensive resource than previous versions, and the identification of a large number of SSRs has great potential for advancing genetic research on *E. nutans*.

4.2. SSR Validation and Genetic Analysis

An understanding of genetic diversity and population structure is crucial for the effective management and utilization of germplasm resources, as well as for accelerating the progress of forage breeding. Previous studies on germplasm evaluation of *E. nutans* using SSR markers revealed a high level of genetic diversity among wild germplasm from Tibet and Sichuan, with a mean genetic similarity coefficient of 0.719. The markers used in this study were obtained from wheat and *Elymus* species and had an average PPB and PIC of 91.38% and 0.224, respectively [13]. In the present study, 17 polymorphic EST-SSR markers were used to evaluate the genetic variation of *E. nutans* accessions sampled from eastern Tibet and showed a similar level of genetic diversity (genetic similarity coefficient = 0.729). The average PPB and PIC values of all markers were 88% and 0.424, respectively. These results suggest a wide genetic background for *E. nutans*, and the higher PIC value indicates that the SSR markers developed in this study are well suited for use in this species.

In the investigation of the genetic basis, accessions from Qamdo and Nyingchi were distributed across multiple clusters, while accessions from Lhasa and Nagqu showed a pure origin and formed the first cluster. This heterogeneity in genetics may be attributed to the diverse geomorphology and climatic conditions of the QTP [43], highlighting the importance of understanding the impact of environmental factors on the genetic diversity of this species. Further studies exploring the genetic variability of *E. nutans* will provide valuable insights for the effective management and utilization of germplasm resources. In our previous studies of the genetic diversity of *E. breviaristatus*, the population in Qamdo had the highest level of genetic diversity, whereas the population in Lhasa had the lowest [32]; this difference may be due to selection pressures from different habitats. This result is relevant not only to these two species but also to other *Elymus* plants in the QTP and provides important insights for the preservation and utilization of germplasm resources. The large genetic variation in *Elymus* plants in the Qamdo region highlights its importance as a center for germplasm collection, while the need to protect germplasm in the Lhasa region is pressing.

4.3. Phenotypic Variation and Association Analysis

In addition to genetic diversity, plant biomass and seed yield are also key germplasm resource evaluation indicators for forage species. In this study, we aimed to evaluate the phenotypic diversity of *E. nutans*, with a focus on inflorescence traits and seed shattering. We found a high level of phenotypic diversity, with a mean coefficient of variation (CV) of 19.45% among the 31 populations. Similar results were found in a previous study by Zhang et al. [44], in which the phenotypic diversity of 37 *E. nutans* and 36 *E. sibiricus* accessions from the QTP and Mongolia Plateau in China was analyzed using 15 morphological traits. The results showed that *E. nutans* and *E. sibiricus* accessions exhibited 12.67% and 17.10% phenotypic variations, respectively. These traits may be useful for the evaluation of germplasm resources in the *Elymus* genus and even for the description of the genetic relationship among species.

However, to date, there have been few studies on the molecular markers associated with *E. nutans* traits [25], despite this method has been widely applied on crops, such

as soybean, barley, and maize [45–47]. Our association analysis revealed the presence of 11 loci that showed significant association with the traits studied ($p < 0.01$). Two loci amplified by marker EN5 were found to be significantly associated with seven traits. Although the chromosomal location of these bands could not be determined due to a lack of association mapping, these findings provide valuable information for breeding programs aimed at increasing seed yield and reducing seed-shattering losses in production. Furthermore, our study highlights the significant correlations between certain phenotypes of *E. nutans* and climatic and geographical factors. These results help clarify the ecological and evolutionary basis of population adaptation and differentiation and will inform the design of conservation units and aid in better management of genetic resources.

4.4. How Genotypic and Phenotypic Differentiation Is Affected by Geography and Environment

A growing number of reports over the last decade have aided in the advancement of genetic differentiation pattern theory [48]. As an important factor in the process of local adaptation leading to species formation, genetic differentiation pattern theory has received significant attention across both plant and animal studies. It was previously suggested that the genetic differentiation of *E. nutans* fit the IBD pattern on a small geographic scale; the effective spread distance of *E. nutans* was about 100 km [13]. However, in this study, we attempted to infer the genetic structure of *E. nutans* from 31 localities spread across the climate-sensitive QTP region, and we found that the genetic differentiation of *E. nutans* still conformed to the IBD pattern ($r = 0.575$) over a 600-km range. This phenomenon may be caused by the inconsistency of external interference in different regions, resulting in differences in the range of effective dispersal. In addition, IBE played a significant role in this region ($r = 0.329$), and there was a significant autocorrelation between geographical and climatic distance. Similarly, a previous meta-analysis showed that 27 of 70 (38.57%) phylogeographic studies revealed spatial autocorrelation between IBE and IBD patterns [49]. The significant evidence of IBD and IBE was similar to our previous study of *E. breviaristatus*, a related species of *E. nutans* distributed in the same area, indicating that both isolation patterns have significant restrictions on gene flow. Although we detected only a weak significant effect of genetic distance on phenotypic differentiation, our observations suggest that certain phenotypic traits are related to geographical or climatic factors. These findings align with previous studies that noted that not all phenotypic variations can be fully accounted for by genetic variations [50]. Generally speaking, genetic variation contributes most to phenotypic differentiation.

5. Conclusions

In this study, we utilized Illumina HiSeq platform sequencing and de novo transcriptome assembly of *E. nutans* to obtain EST-SSR markers and gain insights into its genetic differentiation patterns. We obtained 17 EST-SSR markers that revealed polymorphism among 31 accessions from eastern Tibet. The effects of loci and environmental factors on phenotypic changes and genetic differentiation were studied by analyzing the markers in combination with the seed-shattering values and 13 inflorescence phenotypic traits. We found that *E. nutans* had substantial genetic and phenotypic variation, with 11 loci and three environmental conditions significantly correlated with phenotypic traits. Among these markers, primer EN5 was the most effective marker for assessing phenotypic diversity in *E. nutans* populations. In addition, Mantel analysis indicated strong IBE and IBD patterns. Our study sheds light on the crucial role of *E. nutans* germplasm resources in collection, evaluation, protection, and molecular breeding efforts.

Supplementary Materials: The following supporting information can be downloaded at: <https://www.mdpi.com/article/10.3390/agronomy13041004/s1>, Figure S1: The K model in the Structure Harvester website shows ΔK corresponding to K values from 2 to 14; Figure S2: Correlations between 13 phenotypic traits, BTS and environmental conditions; Table S1: Geographic information of 31 *E. nutans* locations; Table S2: Detailed information of EST-SSRs based on the number of nucleotides repeat unit;

Table S3: Characterization of the 17 polymorphic primer pairs in *E. nutans*; Table S4: Genetic diversity of *E. nutans* based on 17 EST-SSRs.

Author Contributions: Conceptualization, J.L. and S.C.; methodology, J.L. and S.C.; software, J.L. and H.T.; validation, W.J. and C.Z.; investigation, J.L., W.J. and H.T.; resources, C.Z.; data curation, C.Z.; writing—original draft preparation, J.L. and H.T.; writing—review and editing, S.C.; supervision, C.Z. and S.C.; funding acquisition, S.C. All authors have read and agreed to the published version of the manuscript.

Funding: This research was funded by the Nation Natural Science Foundation of China (No. 31900280), Double First-Class program of Southwest Minzu University (CX2023017) and Key Laboratory of Superior Forage Germplasm in the Qinghai-Tibetan plateau (2020-ZJ-Y03).

Data Availability Statement: The clean reads were submitted to the NCBI's Sequence Read Archive database under BioProject ID: PRJNA934126.

Conflicts of Interest: The authors declare no conflict of interest.

References

1. Löve, A. Conspectus of Triticeae. *Feddes Repert.* **1984**, *95*, 425–524.
2. Lu, B.R. Meiotic studies of *Elymus nutans* and *Elymus jacquemontii* (Poaceae, Triticeae) and their hybrids with *Pseudoroegneria spicata* and seventeen *Elymus* species. *Plant Syst. Evol.* **1993**, *186*, 193–211. [CrossRef]
3. Yen, C.; Yang, J.L.; Baum, B. Synopsis of *Leymus* Hochst. (Triticeae: Poaceae). *J. Syst. Evol.* **2009**, *47*, 67–86. [CrossRef]
4. Ferdinandez, Y.; Somers, D.J.; Coulman, B.E. Estimating the genetic relationship of hybrid brome grass to smooth brome grass and meadow brome grass using RAPD markers. *Plant Breed.* **2010**, *120*, 149–153. [CrossRef]
5. Wang, R.R.C.; von Bothmer, R.; Dvorak, J.; Fedak, G.; Linde-Laursen, I.; Muramatsu, M. Genome symbols in the Triticeae (Poaceae). In *Proceedings of 2nd International Triticeae Symposium*; Wang, R.R.C., Ed.; Utah State University Publications on Design and Production: Logan, UT, USA, 1994; pp. 29–34.
6. Bor, N.L. *The Grasses of Burma, Ceylon, India and Pakistan*; Pergamon Press: Oxford, UK, 1960.
7. Clayton, W.D.; Harman, K.T.; Williamson, H. GrassBase—The Online World Grass Flora. 2006. Available online: <http://www.kew.org/data/grasses-db.html> (accessed on 15 May 2020).
8. Chen, S.L.; Zhu, G.H. *Elymus L. Flora of China (Poaceae)*; Science Press: Beijing, China; Missouri Botanical Garden: Louis, MO, USA, 2006.
9. Sun, J.; Fu, B.J.; Zhao, W.W.; Liu, S.L.; Liu, G.H.; Zhou, H.K.; Shao, X.Q.; Chen, Y.C.; Zhang, Y. Optimizing grazing exclusion practices to achieve goal 15 of the sustainable development goals in the Tibetan plateau. *Sci. Bull.* **2021**, *66*, 1493–1496. [CrossRef]
10. Lei, Y.T.; Zhao, Y.Y.; Yu, F.; Li, Y.; Dou, Q.W. Development and characterization of 53 polymorphic genomic-SSR markers in Siberian wildrye (*Elymus sibiricus* L.). *Conserv. Genet. Resour.* **2014**, *6*, 861–864. [CrossRef]
11. Shi, N.; Naudiyal, N.; Wang, J.N.; Gaire, N.P.; Wu, Y.; Wei, Y.Q.; He, J.L.; Wang, C.Y. Assessing the impact of climate change on potential distribution of *Meconopsis punicea* and its influence on ecosystem services supply in the southeastern margin of Qinghai-Tibet plateau. *Front. Plant Sci.* **2022**, *12*, 830119. [CrossRef]
12. Kou, Y.X.; Wu, Y.X.; Jia, D.R.; Li, Z.H.; Wang, Y.J. Rang expansion, genetic differentiation, and phenotypic adaption of *Hippophaë neurocarpa* (Elaeagnaceae) on the Qinghai-Tibet Plateau. *J. Syst. Evol.* **2014**, *52*, 303–312. [CrossRef]
13. Chen, S.; Zhang, X.; Ma, X.; Huang, L. Assessment of genetic diversity and differentiation of *Elymus nutans* indigenous to Qinghai-Tibet Plateau using simple sequence repeats markers. *Can. J. Plant. Sci.* **2013**, *93*, 1089–1096. [CrossRef]
14. Chen, S.Y.; Ma, X.; Zhang, X.Q.; Chen, Z.H. Genetic variation and geographical divergence in *Elymus nutans* Griseb. (Poaceae: Triticeae) from West China. *Biochem. Syst. Ecol.* **2009**, *37*, 716–722. [CrossRef]
15. Miao, J.M.; Zhang, X.Q.; Chen, S.Y.; Ma, X.; Chen, Z.H.; Zhong, J.C.; Bai, S.Q. Gliadin analysis of *Elymus nutans* Griseb. from the Qinghai-Tibetan Plateau and Xinjiang, China. *Grassl. Sci.* **2011**, *57*, 127–134. [CrossRef]
16. Yan, X.B.; Guo, Y.X.; Liu, F.Y.; Zhao, C.; Liu, Q.L.; Lu, B.R. Population structure affected by excess gene flow in self-pollinating *Elymus nutans* and *E. burchan-buddae* (Triticeae: Poaceae). *Popul. Ecol.* **2010**, *52*, 233–241. [CrossRef]
17. Karan, M.; Evans, D.S.; Reilly, D.; Schulte, K.; Wright, C.; Innes, D.; Holton, T.A.; Nikles, D.G.; Dickinson, G.R. Rapid microsatellite marker development for African mahogany (*Khaya senegalensis*, Meliaceae) using next-generation sequencing and assessment of its intra-specific genetic diversity. *Mol. Ecol. Resour.* **2012**, *12*, 344–353. [CrossRef]
18. Soler, S.; Gramazio, P.; Figàs, M.R.; Vilanova, S.; Rosa, E.; Llosa, E.R.; Borrás, D.; Plazas, M.; Prohens, J. Genetic structure of *Cannabis sativa* var. *indica* cultivars based on genomic SSR (gSSR) markers: Implications for breeding and germplasm management. *Ind. Crops Prod.* **2017**, *104*, 171–178. [CrossRef]
19. Zhang, Z.; Xie, W.; Zhao, Y.; Zhang, J.; Wang, N.; Ntakirutimana, F.; Yan, J.J.; Wang, Y.R. EST-SSR marker development based on RNA-sequencing of *E. sibiricus* and its application for phylogenetic relationships analysis of seventeen *Elymus* species. *BMC Plant Biol.* **2019**, *19*, 235. [CrossRef]

20. Xiong, Y.; Yang, J.; Xiong, Y.; Zhao, J.; Liu, L.; Liu, W.; Sha, L.N.; Zhou, J.Q.; You, M.H.; Li, D.X.; et al. Full-length transcriptome sequencing analysis and characterization, development and validation of microsatellite markers in *Kengyilia melanthera*. *Front. Plant Sci.* **2022**, *13*, 959042. [[CrossRef](#)]
21. Sun, M.; Dong, Z.X.; Yang, J.; Wu, W.D.; Zhang, C.L.; Zhang, J.B.; Zhao, J.M.; Xiong, Y.; Jia, S.G.; Ma, X. Transcriptomic resources for prairie grass (*Bromus catharticus*): Expressed transcripts, tissue-specific genes, and identification and validation of EST-SSR markers. *BMC Plant Biol.* **2021**, *21*, 264. [[CrossRef](#)]
22. Luo, D.; Zhou, Q.; Ma, L.C.; Xie, W.G.; Wang, Y.R.; Hu, X.W.; Liu, Z.P. Novel polymorphic expressed-sequence tag–simple-sequence repeat markers in *Campeiostrachys nutans* for genetic diversity analyses. *Crop Sci.* **2015**, *55*, 2712–2718. [[CrossRef](#)]
23. Zhao, Y.; Zhang, J.; Zhang, Z.; Xie, W. *Elymus nutans* genes for seed shattering and candidate gene-derived EST-SSR markers for germplasm evaluation. *BMC Plant Biol.* **2019**, *19*, 102. [[CrossRef](#)]
24. Kamali, M.; Samsampour, D.; Bagheri, A.; Mehrafarin, A.; Homaei, A. Association analysis and evaluation of genetic diversity of *Teucrium stocksianum* Boiss. populations using ISSR markers. *Genet. Resour. Crop Evol.* **2023**, *70*, 691–709. [[CrossRef](#)]
25. Yan, H.; Zhang, Y.; Zeng, B.; Yin, G.; Zhang, X.; Ji, Y.; Huang, L.K.; Jiang, X.M.; Liu, X.C.; Peng, Y.; et al. Genetic diversity and association of EST-SSR and SCoT markers with rust traits in Orchardgrass (*Dactylis glomerata* L.). *Molecules* **2016**, *21*, 66. [[CrossRef](#)] [[PubMed](#)]
26. Muhammad, S.; Sajjad, M.; Khan, S.H.; Shahid, M.; Zubair, M.; Awan, F.S.; Khan, A.I.; Mubarak, M.S.; Tahir, A.; Umer, M.; et al. Genome-wide association analysis for stripe rust resistance in spring wheat (*Triticum aestivum* L.) germplasm. *J. Integr. Agric.* **2020**, *19*, 2035–2043. [[CrossRef](#)]
27. Bourne, E.C.; Bocedi, G.; Travis, J.M.J.; Pakeman, R.J.; Brooker, R.W.; Schiffrers, K. Between migration load and evolutionary rescue: Dispersal, adaptation and the response of spatially structured populations to environmental change. *Proc. R. Soc. B Biol. Sci.* **2014**, *281*, 20132795. [[CrossRef](#)] [[PubMed](#)]
28. Wang, I.J.; Summers, K. Genetic structure is correlated with phenotypic divergence rather than geographic isolation in the highly polymorphic strawberry poison-dart frog. *Mol. Ecol.* **2010**, *19*, 447–458. [[CrossRef](#)]
29. Noguerales, V.; Cordero, P.J.; Ortego, J. Hierarchical genetic structure shaped by topography in a narrow-endemic montane grasshopper. *BMC Evol. Biol.* **2016**, *16*, 96. [[CrossRef](#)]
30. Wright, S. Isolation by distance under diverse systems of mating. *Genetics* **1945**, *30*, 571–572. [[CrossRef](#)]
31. Lichstein, J. Multiple regression on distance matrices: A multivariate spatial analysis tool. *Plant Ecol.* **2007**, *188*, 117–131. [[CrossRef](#)]
32. Li, J.; Ma, S.; Jiang, K.; Zhang, C.; Liu, W.; Chen, S. Drivers of population divergence and genetic variation in *Elymus breviaristatus* (Keng) Keng f. (Poaceae: Triticeae), an endemic perennial herb of the Qinghai-Tibet plateau. *Front. Ecol. Evol.* **2022**, *10*, 1068739. [[CrossRef](#)]
33. Marchese, C. Biodiversity hotspots: A shortcut for a more complicated concept. *Glob. Ecol. Conserv.* **2015**, *3*, 297–309. [[CrossRef](#)]
34. Grabherr, M.G.; Haas, B.J.; Yassour, M.; Levin, J.Z.; Thompson, D.A.; Amit, I.; Adiconis, X.; Fan, L.; Raychowdhury, R.; Zeng, Q.D.; et al. Full-length transcriptome assembly from RNA Seq data without a reference genome. *Nat. Biotechnol.* **2011**, *29*, 644–652. [[CrossRef](#)]
35. Thiel, T.; Michalek, W.; Varshney, R.; Graner, A. Exploiting EST databases for the development and characterization of gene-derived SSR-markers in barley (*Hordeum vulgare* L.). *Theor. Appl. Genet.* **2003**, *106*, 411–422. [[CrossRef](#)]
36. Yeh, F.C.; Boyle, T.J.B. Population genetic analysis of co-dominant and dominant markers and quantitative traits. *Belg. J. Bot.* **1997**, *129*, 157–163.
37. Tamura, K.; Stecher, G.; Peterson, D.; Filipiński, A.; Kumar, S. MEGA6: Molecular evolutionary genetics analysis version 6.0. *Mol. Biol. Evol.* **2013**, *30*, 2725–2729. [[CrossRef](#)]
38. Falush, D.; Stephens, M.; Pritchard, J.K. Inference of population structure using multilocus genotype data: Dominant markers and null alleles. *Mol. Ecol. Notes.* **2007**, *7*, 574–578. [[CrossRef](#)]
39. Earl, D.A.; von Holdt, B.M. Structure Harvester: A website and program for visualizing structure output and implementing the Evanno method. *Conserv. Genet. Resour.* **2012**, *4*, 359–361. [[CrossRef](#)]
40. Peakall, R.; Smouse, P.E. GenA1Ex 6.5: Genetic analysis in excel. Population genetic software for teaching and research—An update. *Bioinformatics* **2012**, *28*, 2537–2539. [[CrossRef](#)]
41. Bradbury, P.J.; Zhang, Z.; Kroon, D.E.; Casstevens, T.M.; Ramdoss, R.; Buckler, E.S. TASSEL: Software for association mapping of complex traits in diverse samples. *Bioinformatics* **2007**, *23*, 2633–2635. [[CrossRef](#)]
42. Liu, K.; Xu, H.; Liu, G.; Guan, P.; Zhou, X.; Peng, H.; Yao, Y.; Ni, Z.; Sun, Q.; Du, J. QTL mapping of fag leaf-related traits in wheat (*Triticum aestivum* L.). *Theor. Appl. Genet.* **2018**, *131*, 839–849. [[CrossRef](#)]
43. Yan, X.B.; Guo, Y.X.; Zhou, H.; Lu, B.R.; Wang, K. Genetic patterns of ten *Elymus* species from the Tibetan and Inner Mongolian plateaus of China. *Grass Forage Sci.* **2006**, *61*, 398–404. [[CrossRef](#)]
44. Zhang, Z.; Xie, W.; Zhang, J.; Zhao, X.; Zhao, Y.; Wang, Y. Phenotype- and SSR-based estimates of genetic variation between and within two important *Elymus* species in western and northern China. *Genes* **2018**, *9*, 147. [[CrossRef](#)]
45. Jun, T.H.; Van, K.; Kim, M.Y.; Lee, S.H.; Walker, D.R. Association analysis using SSR markers to find QTL for seed protein content in soybean. *Euphytica* **2008**, *162*, 179–185. [[CrossRef](#)]
46. Azmach, G.; Gedil, M.; Menkir, A.; Spillane, C. Marker-trait association analysis of functional gene markers for provitamin A levels across diverse tropical yellow maize inbred lines. *BMC Plant Biol.* **2013**, *13*, 227. [[CrossRef](#)] [[PubMed](#)]
47. Berger, G.L.; Liu, S.; Hall, M.D.; Brooks, W.S.; Chao, S.; Muehlbauer, G.J.; Baik, B.K.; Steffenson, B.; Griffey, C.A. Marker-trait associations in Virginia Tech winter barley identified using genome-wide mapping. *Theor. Appl. Genet.* **2013**, *126*, 693–710. [[CrossRef](#)] [[PubMed](#)]

48. Castilla, A.R.; Méndez-Vigo, B.; Marcer, A.; Martínez-Minaya, J.; Conesa, D.; Picó, F.X.; Alonso-Blanco, C. Ecological, genetic and evolutionary drivers of regional genetic differentiation in *Arabidopsis thaliana*. *BMC Evol. Biol.* **2020**, *20*, 71. [[CrossRef](#)]
49. Sexton, J.P.; Hangartner, S.B.; Hoffmann, A.A. Genetic isolation by environment or distance: Which pattern of gene flow is most common? *Evolution* **2014**, *68*, 1–15. [[CrossRef](#)]
50. Ghalambor, C.K.; McKay, J.K.; Carroll, S.P.; Reznick, D.N. Adaptive versus non-adaptive phenotypic plasticity and the potential for contemporary adaptation in new environments. *Funct. Ecol.* **2007**, *21*, 394–407. [[CrossRef](#)]

Disclaimer/Publisher’s Note: The statements, opinions and data contained in all publications are solely those of the individual author(s) and contributor(s) and not of MDPI and/or the editor(s). MDPI and/or the editor(s) disclaim responsibility for any injury to people or property resulting from any ideas, methods, instructions or products referred to in the content.